

A multiscale graph cut approach to bright-field multiple cell image segmentation using a Bhattacharyya Measure

Soo Min Kang^a, Justin W.L. Wan^{a,b}

^aCentre for Computational Mathematics in Industry and Commerce, University of Waterloo, Ontario, Canada; ^bDavid R. Cheriton School of Computer Science, University of Waterloo, Ontario, Canada

ABSTRACT

Automatic segmentation of bright-field cell images is important to cell biologists, but is difficult to achieve due to the complex nature of the cells in bright-field images (poor contrast, broken halo, missing boundaries). The standard segmentation techniques, such as the level set method and active contours, are not able to overcome these features of bright-field images. Consequently, poor segmentation results are produced. In this paper, we present a robust segmentation method, which combines the techniques of graph cut, multiresolution, and Bhattacharyya measure, performed in a multiscale framework, to locate multiple cells in bright-field images. The issue of low contrast in bright-field images is addressed by determining the difference in intensity profiles of the cells and the background. The resulting segmentation on the entire image frame provides global information. Then a local segmentation at different regions of interest is performed to obtain finer details of the segmentation result. We illustrate the effectiveness of the method by presenting the segmentation results of C2C12 (muscle) cells in bright-field images.

Keywords: bright-field images, image segmentation, graph cut, Bhattacharyya measure

1. INTRODUCTION

Time-lapse microscopy is an important tool for biologists to study the morphology and behaviour of live cells. Images of the cells are taken at regular intervals for a fixed period of time. Each experiment generates hundreds of image frames, with tens to hundreds of cells in each frame. Manual detection of a cell can be tedious and error prone. Thus, a tracking method, that is robust and automated, has been of great interest in the study of live cells.

Numerous image segmentation techniques, such as snakes,¹ parametric active contours,^{2,3} and level set methods,⁴ have been developed to analyze cells of fluorescent images. The relatively simple shape and bright intensities that fluorescent images exhibit (Figure 1 (left)), allow standard techniques, such as the level set method, to segment cells with high accuracy; see Figure 1 (centre right). However, studies have shown that the chemical agents that are used to produce fluorescent images can cause unwanted damages to the cell. Another known issue with fluorescent images is the occasional disappearance and reappearance of the cells in a sequence of image frames, leading to potentially incorrect tracking of cell behaviour.⁵ Bright-field images, on the other hand, show more details of the cells than fluorescent images (Figure 1 (centre left)). However, the small contrast between the cells and the background, the halo artifacts caused by light microscopy, and the poorly defined cell boundaries, are some of the features of bright-field images of cells that make it challenging to segment; see Figure 1 (right).

There are relatively few segmentation methods for bright-field images, due to the issues as described above. Some previous work on this matter include combining the active contour method with the watershed techniques.⁶ Another approach is based on K-means clustering and spectral partitioning.⁷ Many of these approaches handle images containing a single cell. Segmentation of multiple cells in an image frame pose additional challenges. In a single image frame, different cells have very different shapes and intensity profiles. This makes it difficult for any single model to capture all of the variations that are present on the same image frame. As a result, these cells are often over- (or under-) segmented. One consequence is that nearby cells may be identified as one big blob, rather than individual cells.

For further information, please contact Soo Min Kang: sm2kang@uwaterloo.ca, or Justin W.L. Wan: justin.wan@uwaterloo.ca.

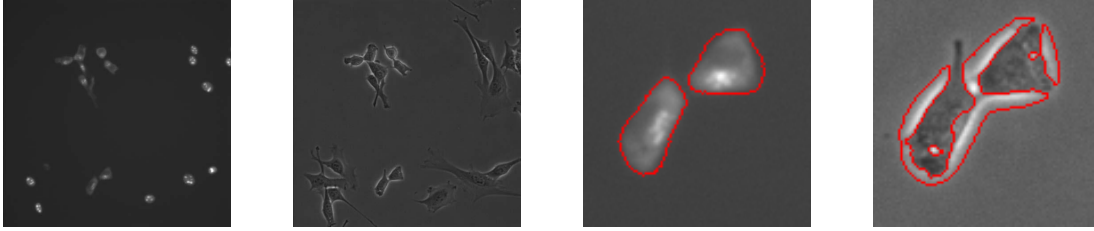


Figure 1: Same cells using (left) fluorescent and (centre left) bright-field imaging. A level set segmentation of a dividing cell from (centre right) fluorescent and (right) bright-field images.

2. METHODOLOGY

The approach presented here consists of two main techniques for bright-field cell segmentation. One is the use of the Bhattacharyya measure with a graph cut algorithm, to address the issue of low contrast in bright-field images. Another is a multiscale framework that we developed, to capture the fine details of multiple cells that result from over-segmentation.

2.1 Segmentation

The segmentation procedure begins with a segmentation of the entire image that contains multiple cells. We capture the difference in intensity profiles by applying the Bhattacharyya measure,⁸ defined as:

$$\mathcal{B}(f, g) = \sum_{z \in \mathcal{Z}} \sqrt{f(z)g(z)},$$

where $f(z)$ and $g(z)$ are two distributions of intensity z in a set of intensity variables \mathcal{Z} . In general, the Bhattacharyya coefficient has a value between 0 and 1, with 0 corresponding to no overlap between the distributions and 1 representing a perfect match. This measure will be incorporated into the segmentation algorithm.

Let p be a pixel and I_p its intensity. Furthermore, let L be a binary array, where $L(p) \in \{0, 1\}$ denotes the label (1 = “background”, 0 = “object”) of p . Due to the issue of low contrast in bright-field images, we observe that the intensities of the cells usually have more variations than the intensities of the background. Thus, we formulate the image segmentation problem by searching for a label L such that the intensity distribution P_{L_1} for the region $L_1 \equiv \{p | L(p) = 1\}$ matches a learned distribution M of the background. Mathematically speaking, the goal is to find an optimal L that would minimize the energy functional:

$$\min_L -\mathcal{B}(P_{L_1}, M). \quad (1)$$

The minimization of (1), however, is computationally expensive and difficult to solve. Thus, we transform (1) into a graph cut segmentation problem:

$$\min_L R(L) + \lambda \cdot S(L), \quad (2)$$

where $R(L) = \sum_{p \in P} R_p(L(p))$ and $S(L) = \sum_{\{p,q\} \in N} S_{\{p,q\}}$ represent the regional and smoothness terms, respectively, in an \mathcal{N} set of neighbouring node pairs. The presence of the $\lambda \geq 0$ parameter in (2) allow users to specify the relative importance of the smoothness property from the regional property. The regional property incorporates the Bhattacharyya measure by defining $R(L)$ as:

$$R(L) = (1 - \alpha) \sum_{p \in R_0^L} \frac{-\mathcal{B}(P_{L_1}, M)}{A_{L_1}} + \sum_{p \in R_1^L} L(p) \left(\frac{-\mathcal{B}(P_{L_1}, M)}{A_{L_1}} + \sum_{z \in \mathcal{Z}} \frac{K_z(I_p)}{A_{L_1}} \sqrt{\frac{M(z)}{P_L(z)}} \right), \quad (3)$$

where $\alpha \in [0, 1]$ is some constant, A_{L_1} is the area of L_1 , and K_z is the Gaussian kernel,

$$K_z(I_p) = \frac{1}{\sqrt{2\pi\omega^2}} e^{-\frac{(z-I_p)^2}{2\omega^2}} \quad \forall z \in \mathcal{Z},$$

with $\omega > 0$ representing the width of the kernel. The smoothness term $S(L)$ in (2), again, is defined using the Gaussian distribution:⁹

$$S(L) = \sum_{\{p,q\} \in \mathcal{N}} \frac{1}{\|p - q\|} e^{-\frac{(I_p - I_q)^2}{2\sigma^2}}, \quad (4)$$

with the constant $\sigma > 0$ determining the smoothness of the distribution.

The two terms that are used to define the regional property in (3), measures the likelihood of the pixels connected to the object and background, respectively. The graph cut segmentation defines edge weights $w_{\{s,p\}}$ and $w_{\{q,t\}}$ with a source node s (object) and a sink node t (background), respectively, using these two terms. Together with the weights $w_{\{p,q\}}$ that are assigned between the nodes, which are represented by the smoothness term $S(L)$, a graph cut based on the min-cut/max-flow algorithm is able to separate the pixels of the cells from the background; see Figure 2.

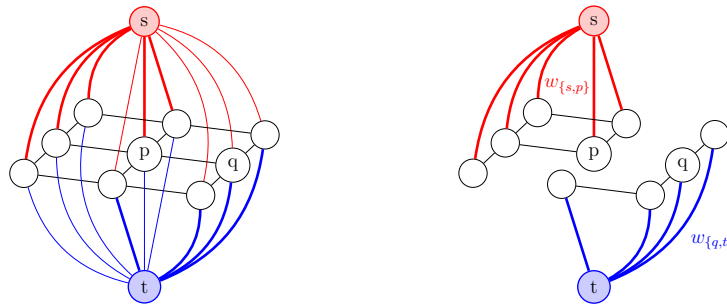


Figure 2: The min-cut/max-flow algorithm cuts the graph based on the relative edge weights $w_{\{s,p\}}$ and $w_{\{q,t\}}$.

Despite the conversion into a graph cut segmentation problem, (2) remains to be a computationally expensive optimization problem to solve. Thus, we follow Ayed et al.'s approach,⁸ and compute a sequence of labels $\{L^{n+1}\}$, which are the solutions to the minimization problems parametrized by α_n :

$$L^{n+1} = \arg \min_L \left\{ (1 - \alpha_n) \sum_{p \in L_0} \frac{-\mathcal{B}(P_{L^n}, M)}{A_{L_1^n}} + \sum_{p \in L_1} L^n(p) \left(\frac{-\mathcal{B}(P_{L^n}, M)}{A_{L_1^n}} + \sum_{z \in Z} \frac{K_z(I_p)}{A_{L_1^n}} \sqrt{\frac{M(z)}{P_{L^n}(z)}} \right) + \lambda S(L) \right\}. \quad (5)$$

The labels L^n of (5) converge to the solution of (1) as $\alpha_n \rightarrow 0$; see paper by Ayed et al. for proof of convergence. The principle steps that are involved in the Bhattacharyya measure based graph-cut segmentation is outlined in Table 1.

2.2 Multiscale segmentation

Experiments revealed that applying the algorithm presented by Ayed et al. on bright-field images containing multiple cells often resulted in over-segmentation. We found that segmenting these images in multiscale fashion would overcome this problem. In our algorithm, we refer to the application of the Bhattacharyya measure based graph cut segmentation on a whole bright-field image as **global segmentation**. In global segmentation, the main features of the image are revealed as cell blobs. Some of these blobs are isolated cells, and some are groups of cells that are located close together. Each blob from global segmentation is segmented individually to obtain the fine details of the cells. This step of refinement is referred to as **local segmentation**.

The main idea of multiscale segmentation is to “zoom in” at each of the cell blobs after every segmentation. More precisely, after global segmentation, each connected piece is identified and fitted into a local rectangular

Table 1: Main Algorithm. L^{n+1} in the optimization step can be computed in low-order polynomial time using the max-flow algorithm of Boykov and Kolmogorov.¹⁰

Main Algorithm	
1.	Initialize L^n : set $L_p^n = L_p^0 = 1 \forall p \in \mathcal{P}$
2.	Initialize α_n : set $\alpha_n = \alpha_0$ with $0 < \alpha_0 < 1$
3.	Optimize L : $L^{n+1} = \arg \min_L \lambda \sum_{\{p,q\} \in \mathcal{N}} w_{\{p,q\}} + \sum_{p \in R_0^{L^n}} w_{\{s,p\}} + \sum_{p \in R_1^{L^n}} w_{\{p,t\}}$
4.	If $L^n \neq L^{n+1}$,
i)	Set $n = n + 1$
ii)	Decrease α_n by a factor of ρ : $\alpha_n = \alpha_{n-1}^\rho$ for some constant $\rho > 1$
iii)	Repeat from step 3
	If $L^n = L^{n+1}$,
i)	Terminate. L^{n+1} is the final mask of the image.

region (region of interest). The Bhattacharyya measure based graph cut segmentation is applied to each of the local regions of interest again. If a blob from global segmentation contains a single cell, then the local segmentation step is able to obtain a more precise result. If the blob contains multiple non-overlapping cells, then the algorithm is able to separate these cells, due to change in scale. As a result, through the use of multiscale segmentation technique, the graph cut segmentation algorithm is able to segment cells with high precision and separate nearby cells.

For each cell blob, one may apply local segmentation recursively; i.e. for each new connected piece discovered, an additional graph cut segmentation step can be applied. One may think of it as a telescopic zoom-in process. In our experiments, only one local segmentation was performed because it produced sufficient results. The final segmentation result is obtained by combining all the local segmentation results onto the original image frame. The series of steps that are involved in the multiscale algorithm can be visualized in Figure 3.

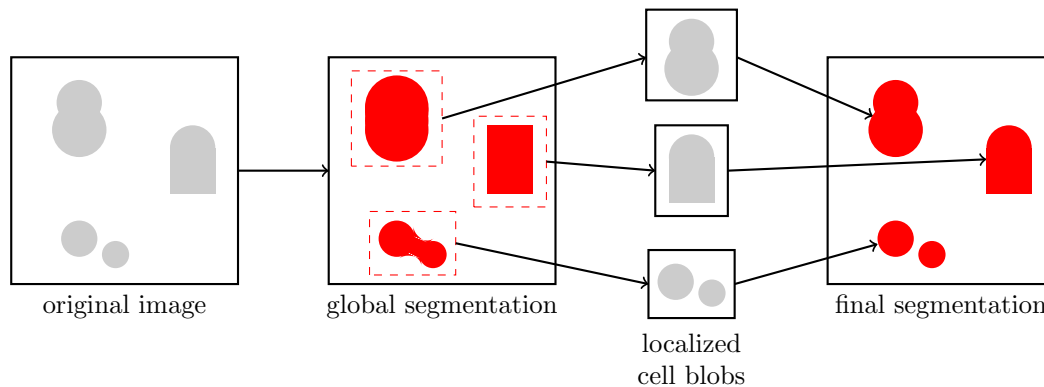


Figure 3: A schematic diagram of the multiscale algorithm. Grey objects represent the cells in a given image. Red objects represent the “object” mask. Red-dashed boxes are the local regions to be used for local segmentation.

3. NUMERICAL RESULTS

The proposed segmentation algorithm is applied to bright-field cell images with live C2C12 (muscle) cells obtained from experiments performed at the Genomic Laboratory, McGill University. All computations were done using MATLAB on a MAC with a 2.7GHz processor. The size of the image frame is 512×512 . However, it was found that the Bhattacharyya measure based graph cut segmentation on lower resolution images, down-sampled from the original image frame, improved the quality of the segmentation; see Figure 4. Experiments presented here

were performed on a lower resolution image (1/4 of its original size) from the original 512×512 image frame. The learned distributions M were obtained by measuring the frequency count of the intensities on the border of the image of interest. Images whose borders contained cells, had to be excluded manually when obtaining M .

Quantitative results were evaluated by calculating the percentage of the pixels that were correctly classified when compared to the ground truth. That is, $\text{accuracy} = |L \cap L_{\text{true}}|/|L|$, where L denotes the segmentation result from the proposed multiscale algorithm, and L_{true} is the ground truth, which can be computed using manual segmentation.

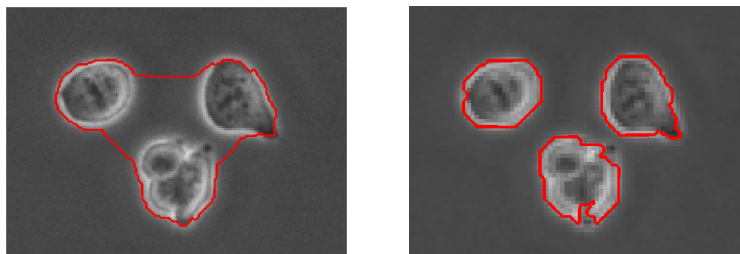


Figure 4: Multi-resolution segmentation comparison. Left: The Bhattacharyya measure graph cut segmentation applied to cells cropped from a 512×512 image. Right: Segmentation technique applied to cells cropped from a 256×256 image.

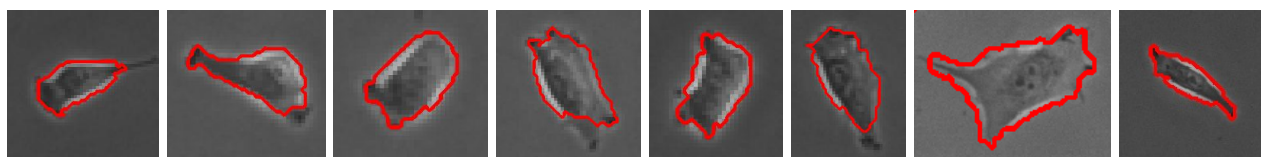


Figure 5: Segmentation results of the graph cut algorithm using the Bhattacharyya measure.

Figure 5 shows the results of the graph cut segmentation using the Bhattacharyya measure on a set of images with different shapes of cells. The segmentation algorithm is able to capture cell images of low contrast.

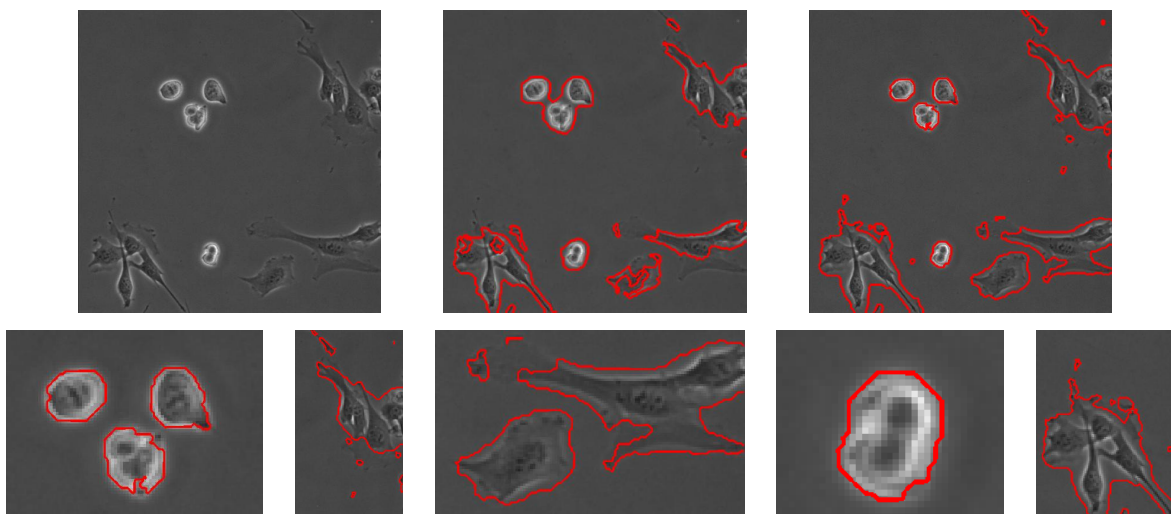


Figure 6: (Top left) The given image frame, (top centre) initial segmentation, (top right) final segmentation), (bottom) segmentations of five cell blobs.

Figure 6 illustrates the process of the multiscale segmentation on an image frame (top left). First, a global

scale segmentation is performed on the image frame; see Figure 6 (top centre). It shows that the global segmentation step is able to identify the five major regions of the image where cells exist. However, the cell boundaries are not very precise and nearby cells are identified as one big blob. In the local segmentation step, each cell blob from global segmentation is segmented locally; see Figure 6 (bottom row). Specifically, it can be seen that the three nearby cells are segmented as a single blob in global segmentation, but identified as three individual cells in local segmentation; see Figure 6 (bottom left). The final segmentation result shown in Figure 6 (top right) has an accuracy of 92.89%.

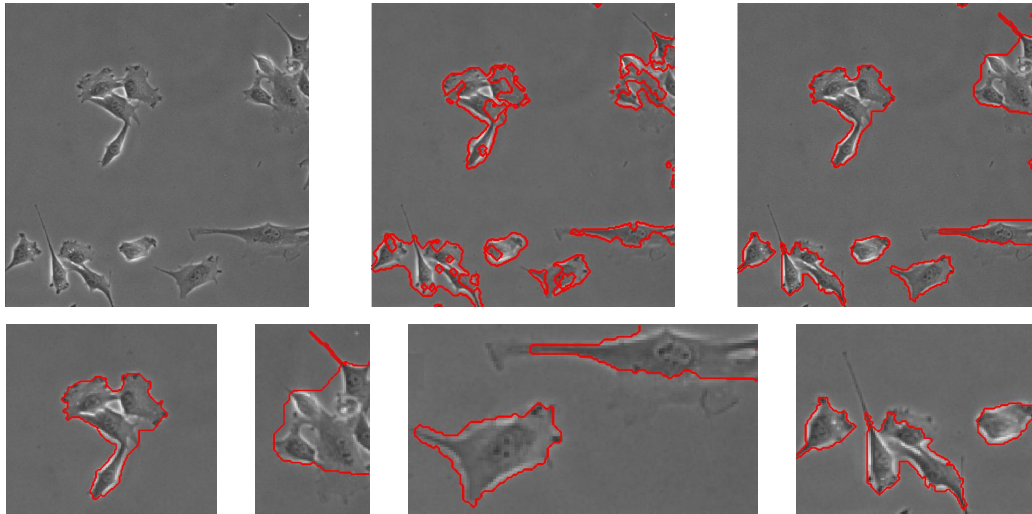


Figure 7: Results of the multiscale graph cut segmentation algorithm on image frames with multiple cells.

Figure 7, also, illustrates the multiscale segmentation algorithm. The global segmentation step (top centre) is able to identify four blobs using the Bhattacharyya measure based graph cut segmentation method. Again, the boundaries that are obtained via global segmentation are not very precise, especially those cells with low contrast. However, local segmentation is able to identify the boundaries of the poorly contrasted cells in a well-defined manner (bottom centre right). The final mask (top right) has an accuracy of 92.55%.

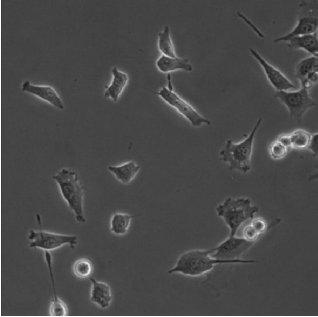
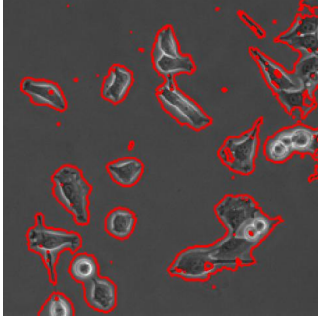
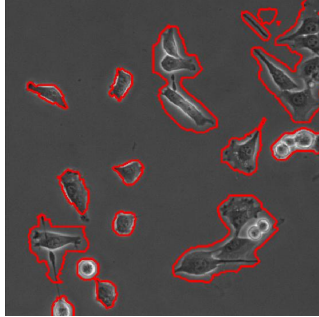
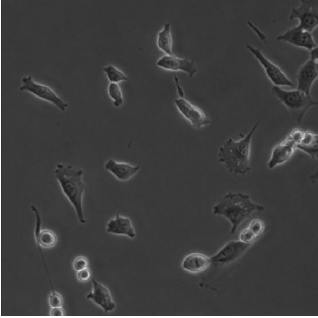
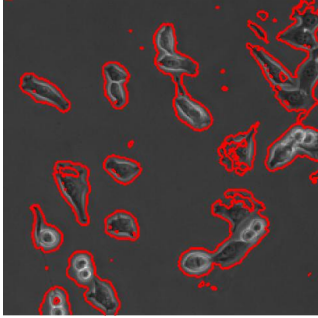
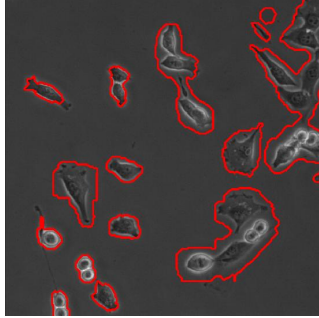
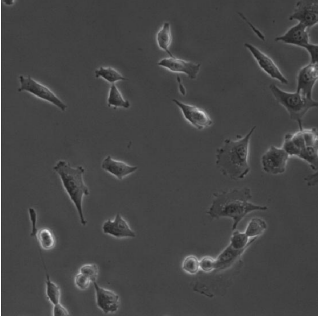
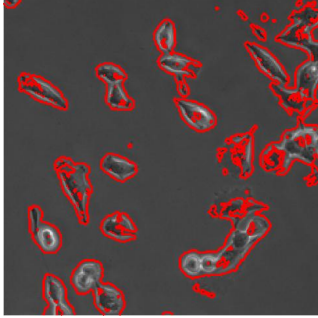
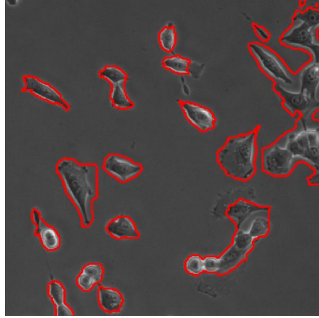
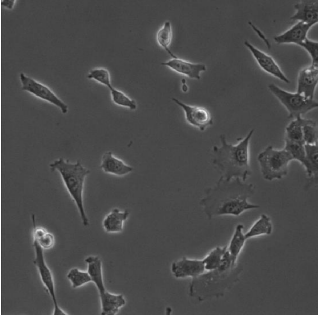
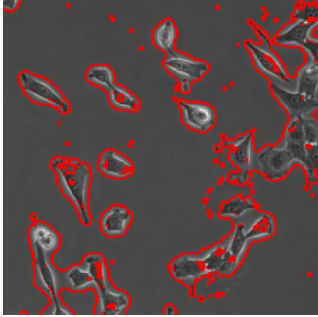
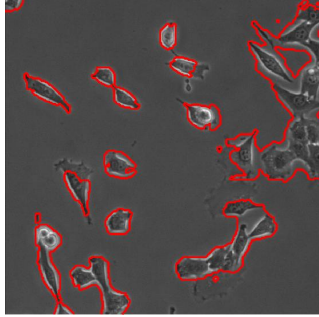
Table 2 displays the segmentation results of a sequence of frames in a single experiment. It illustrates the ability of the algorithm to track the activity of the cells. Each frame is segmented independent of one another.

We note that when the contrast of the cell is very low, sometimes under-segmentation and sometimes over-segmentation occur. In general, the algorithm does a good job of segmenting non-overlapping cells, even if they may be close to one another. The segmentation results can be further improved by providing more information to its initial mask. That is, instead of providing a mask, which is entirely labelled as 1s in step 1 of the algorithm outlined in Table 1, providing some “hard constraints” prior to segmentation can improve results. This can be done by manually identifying some cells as “object,” or by using the segmentation result from previous frames as the initial mask of the current frame.

4. CONCLUSION

We have presented a robust segmentation method which is based on a multiscale framework. The global segmentation step performs a graph cut method that is able to extract cells from the low contrast background by utilizing the Bhattacharyya measure. We have explained how cells grouped as a blob can be resolved by a “zoom-in” process, the local segmentation step. Segmentation results of live cell images have been presented. Future work includes further investigation in identifying individual cells that overlap one another.

Table 2: Sequence of frames segmented using the multiscale segmentation algorithm.

Original Image	Global Segmentation	Final Segmentation
		
		
		
		

ACKNOWLEDGMENTS

The authors would like to thank Robert Sladek and Haig Djambazian from the Department of Medicine and Human Genetics at McGill University for the provision of the C2C12 microscopy images. This work was supported by the National Sciences and Engineering Research Council of Canada.

REFERENCES

- [1] Kass, M., Witkin, A., and Terzopoulos, D., "Snakes: Active contour models," *Int. J. Comput. Vision* **1**, 321–331 (1988).
- [2] Zimmer, C., Labruyere, E., Meas-Yedid, V., Guillen, N., and Olivo-Marin, J., "Segmentation and tracking of migrating cells in videomicroscopy with parametric active contours: A tool for cell-based drug testing," *IEEE Transactions on Medical Imaging* **21**, 1212–1221 (2002).
- [3] Zimmer, C. and Olivo-Marin, J. C., "Coupled parametric active contours," *IEEE Transactions on Pattern Analysis and Machine Intelligence* **27**, 1838–1842 (2005).
- [4] Zhang, B., Zimmer, C., and Olivo-Marin, J., "Tracking fluorescent cells with coupled geometric active contours," in [*Proceedings of IEEE International Symposium on Biomedical Imaging*], 476–479 (2004).
- [5] Dzyubachyk, O., van Cappellen, W., Esser, J., Niessen, W., and Meijering, E., "Advanced level-set-based cell tracking in time-lapse fluorescence microscopy," *IEEE Transactions on Medical Imaging* **29**, 852–867 (2010).
- [6] Tse, T., Bradbury, L., Wan, J., Djambazian, H., Sladek, R., and Hudson, T., "A combined watershed and level set method for segmentation of brightfield cell images," *Proceedings of SPIE Symposium on Medical Imaging: Image Processing* **7259** (2009).
- [7] Bradbury, L. and Wan, J., "A spectral K-means approach to bright-field cell image segmentation," *32nd Annual International Conference of the IEEE EMBS* (2010).
- [8] Ayed, I., Chen, H., Punithakumar, K., Ross, I., and Li, S., "Graph cut segmentation with a global constraint: Recovering region distribution via a bound of the Bhattacharyya measure," *IEEE International Conference on Computer Vision and Pattern Recognition*, 1–7 (2010).
- [9] Boykov, Y. and Funka-Lea, G., "Graph cuts and efficient N-D image segmentation," *International Journal of Computer vision* **70**(2), 109–131 (2006).
- [10] Boykov, Y. and Kolmogorov, V., "An experimental comparison of min-cut/max-flow algorithms for energy minimization in vision," *IEEE Transactions on PAMI* **26**, 1124–1137 (2004).